Iran J Nucl Med. 2023;31(1):20-28 [Serial No. 60]

Homepage: https://irjnm.tums.ac.ir/

ORIGINAL RESEARCH ARTICLE

Production of radioimmunoPET grade zirconium-89

Fatemeh Mohammadpour-Ghazi, Hassan Yousefnia, Samaneh Zolghadri, Mohammad Yarmohammadi, Behrouz Alirezapour, Ali Rahiminejad, Gholamreza Aslani

Radiation Application Research School, Nuclear Science and Technology Research Institute, Tehran, Iran

ARTICLE INFO

Article History:
Received: 13 June 2022
Revised: 21 August 2022
Accepted: 23 August 2022
Published Online: 10 October 2022

Keyword:
Zirconium-89
Production
Radiolabeled compounds
Cyclotron

*Corresponding Author:
Hassan Yousefnia, PhD
Address: Radiation Application Research School, Nuclear Science and Technology Research Institute (NSTRI), Tehran, Iran, Postal code: 14155-1339
Email: hyousefnia@aeoi.aeoi.org.ir

ABSTRACT

Introduction: Particular characteristics of ^{89}Zr to produce various labeled compounds are crucial for developing radioimmunopharmaceuticals for clinical trials. This study aimed to produce ^{89}Zr for radiolabeling purposes as radioimmunoPET grade precursor.

Methods: The computational calculations for ^{89}Zr production via ^{89}Y(p,n)^{89}Zr reaction were performed using TALYS-1.8 and ALICE-91. ^{89}Zr was produced by the proton bombardment of the yttrium pellet using a 30 MeV cyclotron. ZR resin was used for the separation of ^{89}Zr from the target. The radionuclidic purity was assessed by a high purity germanium detector. The inductively coupled plasma spectrometry and instant thin layer chromatography methods were considered for chemical and radiochemical purity assessments, respectively. The biodistribution of [^{89}Zr]Zr-oxalate was studied in Wistar rats by both sacrification and imaging. [^{89}Zr]Zr-DFO-trastuzumab was produced as a proof of concept for a radioimmunoPET labeling.

Results: Considering the cross-section of ^{89}Y(p,n)^{89}Zr reaction, 14 MeV proton energy was selected for ^{89}Zr production, while the yttrium pellet target was irradiated at least for 125 µAh,. ^{89}Zr was finally prepared with a yield of 25.9±1.48 MBq/µAh, a specific activity of 344.1 MBq/µg, the radionuclidic and radiochemical purity higher than 99.99% and 99%, respectively. Total amount of the metal ions in the final solution was less than 0.1 ppm. Biodistribution of [^{89}Zr]Zr-oxalate demonstrated high accumulation in the bone, lungs, and heart. [^{89}Zr]Zr-DFO-trastuzumab was produced with a radiochemical purity higher than 99% and specific activity of 74 GBq/g in about 2 hours.

Conclusion: [^{89}Zr]Zr-oxalate was produced with suitable activity and high purity for the preparation of the radioimmunopharmaceuticals.

Use your device to scan and read the article online

How to cite this article: Mohammadpour-Ghazi F, Yousefnia H, Zolghadri S, Yarmohammadi M, Alirezapour B, Rahiminejad A, Aslani G. Production of radioimmunoPET grade zirconium-89. Iran J Nucl Med. 2023;31(1):20-28.

https://doi.org/10.22034/IRJNM.2022.40035

INTRODUCTION

Radionuclides have found many applications in various fields, especially in medicine [1-2]. While short half-life radionuclides such as ^{11}C, ^{18}F, ^{68}Ga, etc., are used in typical positron emission tomography (PET) procedures [3–5], long-term PET studies such as kinetics of antibodies are not possible with these PET radionuclides. Radiolabeled antibodies have been used for tumor detection for over 40 years and are now being developed as an interesting field for molecular imaging [6-7]. Today; a method, sometimes termed immunoPET, combines the high antigen specificity of monoclonal antibodies (mAbs) with the high sensitivity of PET imaging to provide high-quality molecular imaging of a wide range of tumors and other diseases.

Special physical properties of ^{89}Zr ($T_{1/2}$ = 78.41 h, EC = 76.6%, β^+ = 22.3%, $E_{max}(\beta^+)$ = 897 keV, $E_{ave}(\beta^+)$= 397 keV, $R_{ave}(\beta^+)$ = 1.18 mm, E_γ = 908.9 keV, I_γ =100%) [8-9] make this radioisotope an ideal candidate for immunoPET [10-12]. Despite the relatively long half-life of ^{89}Zr, which is consistent with the pharmacokinetics of mAbs, the low-energy positrons of this radionuclide produce high-resolution PET images. Also; safer handling of ^{89}Zr-based radioligands with more in vivo stability as well as higher image resolution and lower absorbed dose rather than ^{124}I-based radioligands, makes this radionuclide a better candidate for immunoPET imaging [13].

Different radiolabeled compounds of ^{89}Zr have shown promising results for the diagnosis of different tumor types. Clinical trials based on ^{89}Zr-radiopharmaceuticals have been reported utilizing trastuzumab, bevacizumab, cetuximab, rituximab, NMOTO53OA, ibritumomab-tiuxetan, cmAb U36 and Hu-J591 MoAb [14]. These studies indicated high tumor uptake, high spatial resolution images, and an excellent signal-to-noise ratio, which make ^{89}Zr-based radioimmunopharmaceuticals as the superior imaging modalities to visualize tumor-associated antigens [13].

Among the methods available for producing zirconium-89, this radionuclide is mainly produced using the bombardment of mono-isotopic natural yttrium at a biomedical cyclotron via $^{89}Y(p,n)^{89}Zr$ nuclear reaction [15-16]. Recently; ^{89}Zr was experimentally produced on a small scale (with a maximum activity of 74 MBq) in the country [15], however, chemical and radiochemical purities have not reported. Use of this radionuclide for nuclear medicine imaging purposes requires its production with high chemical, radiochemical, and radionuclide purities and a suitable activity for labeling with antibodies, peptides, or other small molecules.

Due to the special physical characteristics of ^{89}Zr, this new emerging radioisotope has found an essential role for developing novel imaging agents for immunoPET procedures. This study aimed to produce [^{89}Zr]Zr-oxalate with suitable purity and specific activity for the labeling of the monoclonal antibodies.

METHODS

TALYS-1.8 and ALICE-91 codes were utilized for computational studies. ^{89}Zr was produced using 30 MeV Cyclotron (Cyclone-30, IBA, Belgium). ZR resin was purchased from TrisKem Co. (France). Y_2O_3 powder (99.99% trace metals basis) and all other chemical reagents were provided from Sigma Aldrich (Heidelberg, Germany). Trastuzumab and p-SCN-Bn-Deferoxamine (DFO) were provided from Ariogen Pharmed Co. (Iran) and Macrocyclics Inc. (USA), respectively. Radio-chromatography was performed using Whatman No. 1 paper (Whatman, U.K.) and a thin layer chromatography scanner (Bioscan AR2000, Paris, France). The activity of the samples was measured by a N-type coaxial high purity germanium (HPGe) detector (NIGC-4020) coupled with a multichannel analyzer card system (NIGC1040-, DSG, GMBH). ICP-OES (Turbo-AX-150-Liberty, Varian Co.) was utilized to investigate the chemical purity. The Student's T-test was used to compare the data based on statistical significance defined as $P < 0.05$.

Computational studies

The cross-section of $^{89}Y(p,n)^{89}Zr$ reaction was calculated using TALYS-1.8 and ALICE-91 codes to determine the optimum energy range for ^{89}Zr production. For this purpose, the level density model was employed to calculate the cross-section.

Experimental studies

Preparation and irradiation of yttrium target

To make the target, Y_2O_3 powder (330 mg) was placed into an aluminum pellet with a diameter and thickness of 11 and 0.8 mm, respectively, and pressed under a pressure of 10 tons/cm^2 and finally covered by a high-purity aluminum foil. ^{89}Zr was produced by the bombardment of $^{89}Y_2O_3$ pellet target with 14 MeV proton energy for five hours with the current of 25 μA. Then; the target was washed with 6 M HCl solution as the primary solvent. The experiment was repeated five times.

Separation of ^{89}Zr from the irradiated target

ZR resin (TrisKem) was utilized to separate the ^{89}Zr from the ^{nat}Y target and the other possible impurities. About 200 mg of ZR resin was packed as a separation column for 0.33 g of ^{89}Y oxide pellet. 6 M HCl was applied for conditioning of the column. The column was washed with 2.5 mL of HCl solution and 2.5 mL of water four times, and then [^{89}Zr]Zr-oxalate was obtained in 1.5 mL of 1.0 M oxalic acid solution.

Radionuclide purity and yield measurement

A calibrated HPGe detector was used to investigate the radionuclide purity of the produced radionuclide. The activity of each sample was obtained by measuring the area below the energy peak of 908.9 keV gamma ray according to Equation (2) [17].

$$A = \frac{N}{\varepsilon\, \gamma\, ts\, k1\, k2\, k3\, k4\, k5} \quad (2)$$

Where, ε is the efficiency at photopeak energy, γ is the emission probability of the gamma line corresponding to the peak energy, t_s is the live time of the sample spectrum collection in seconds, m is the mass (kg) of the measured sample, k_1, k_2, k_3, k_4 and k_5 are the correction factors for the nuclide decay from the time the sample is collected to start the measurement, the nuclide decay during counting period, self-attenuation in the measured sample, pulses loss due to random summing and the coincidence, respectively. Where, N is the corrected net peak area of the corresponding photo-peak given as:

$$N = Ns\frac{ts}{tb}\, Nb \quad (3)$$

Where, N_s is the net peak area in the sample spectrum, N_b is the corresponding net peak area in the background spectrum, and t_s is the live time of the background spectrum collection in seconds.

Chemical and radiochemical purities

ICP-OES method was utilized to determine the presence of any chemical impurity in the final solution. Radiochemical purity was investigated using the instant thin layer chromatography method (ITLC). While, Whatman paper was selected as the stationary phase, 20 mM citric acid was applied as the mobile phase.

Biodistribution studies of [^{89}Zr]Zr-oxalate in Wistar rats

100 µL of the radiolabeled compound was injected into the Wistar rats via their tail vein, and its biodistribution was studied for up to 48 h. The injected dose per gram (% ID/g) for each organ was calculated after the activity measurement using the N-type coaxial HPGe detector.

Four rats were considered for each time interval. All values were expressed as mean ± standard deviation (Mean ± SD), and the data were compared using Student's T-test. P values of < 0.05 were considered statistically significant.

Imaging studies

5.55 MBq of the final [^{89}Zr]Zr-oxalate solution was injected intravenously into the Wistar rats through their tail veins. Images were taken 2, 24, 48, and 72 hours after administration of the radiopharmaceutical by a dual-head SPECT system. The rat-to-high-energy-septa distance and the useful field of view (UFOV) were considered 12 cm and 540 mm × 400 mm, respectively.

Preparation and quality control of [^{89}Zr]Zr-DFO-trastuzumab

[^{89}Zr]Zr-DFO-trastuzumab was produced according to the previously reported literature with slight modifications [18]. In the first stage, DFO was conjugated with trastuzumab at 37°C for 30 min while the pH was adjusted to 9, and the chelator: mAb ratio was considered 10:1. [^{89}Zr]Zr-DFO-trastuzumab was prepared at the following conditions: ^{89}Zr/mAb ratio of 2 mCi:1 mg, temperature= 37°C, pH =7 and time=1 h. The radiochemical purity of the compound was determined by the RTLC method using 20 mM citric acid (pH 5).

RESULTS

Computational studies

The cross sections (mb) of different radioisotopes produced in the ^{89}Y(p,x) reaction (calculated by TALYS-1.8 and ALICE-91 codes) are demonstrated in Figures 1 and 2. Also, Figure 3 compares the cross sections of ^{89}Y(p,n)^{89}Zr using ALICE and TALYS codes.

Radionuclide purity and yield measurement

Gamma-ray spectrometry was used to measure and quantify radionuclide impurities. The gamma spectrometry of the ^{89}Zr produced in this study is indicated in Figure 4. As shown in this figure, two significant photons are observed originating from ^{89}Zr. The radionuclide purity of the radioisotope was higher than 99.99%. ^{89}Zr was produced with a yield of 0.70±0.04 mCi/µA.h and a specific activity of 344.1 MBq/µg.

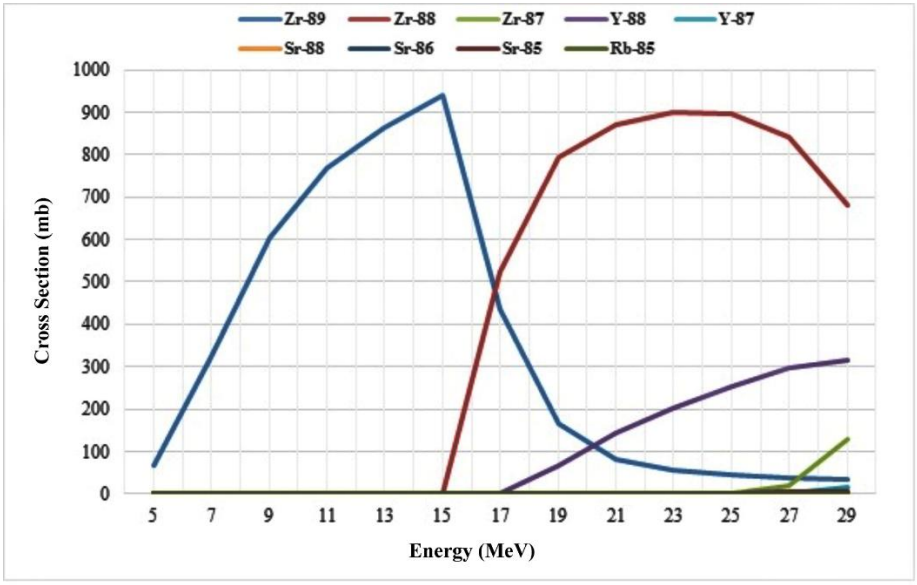

Fig 1. Cross section (mb) of various radionuclides in ^{89}Y(p,x) reaction versus proton energy(MeV), calculated by the ALICE-91 code

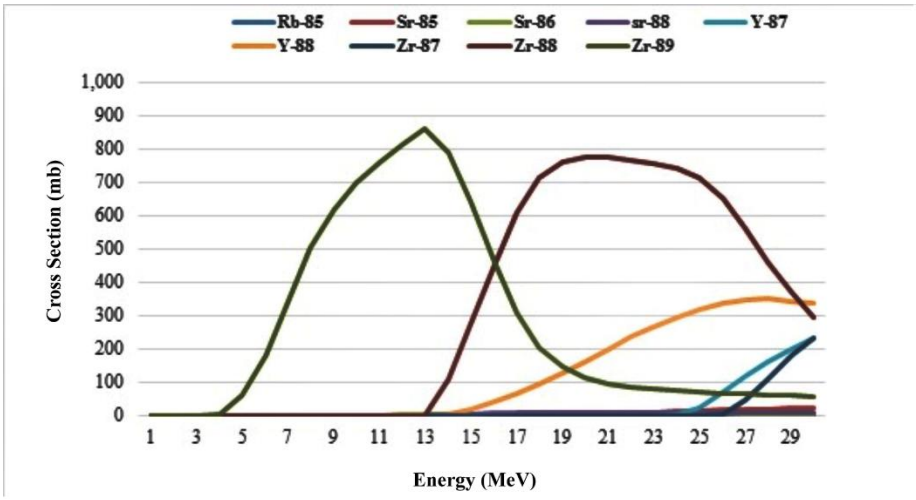

Fig 2. Cross section (mb) of various radionuclides in ^{89}Y(p,x) reaction versus proton energy(MeV), calculated by the TALYS-1.8 code

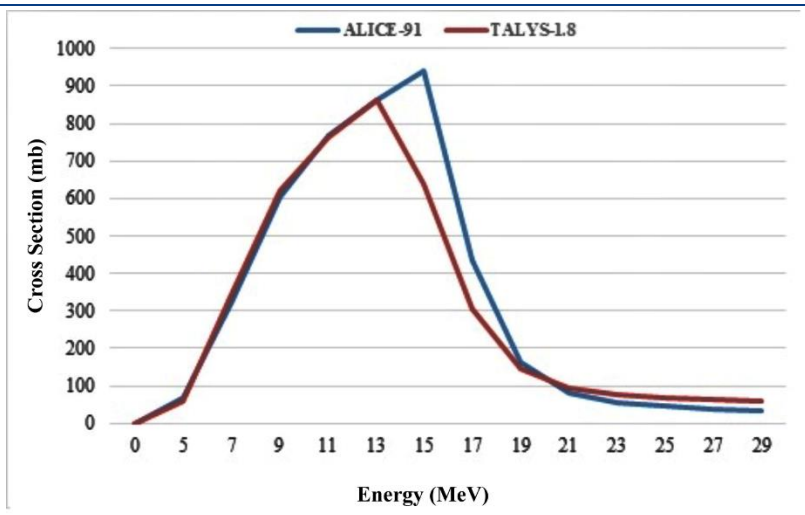

Fig 3. Cross section of ^{89}Y(p,n) ^{89}Zr reaction by Alice-91 and TALYS-1.8 codes

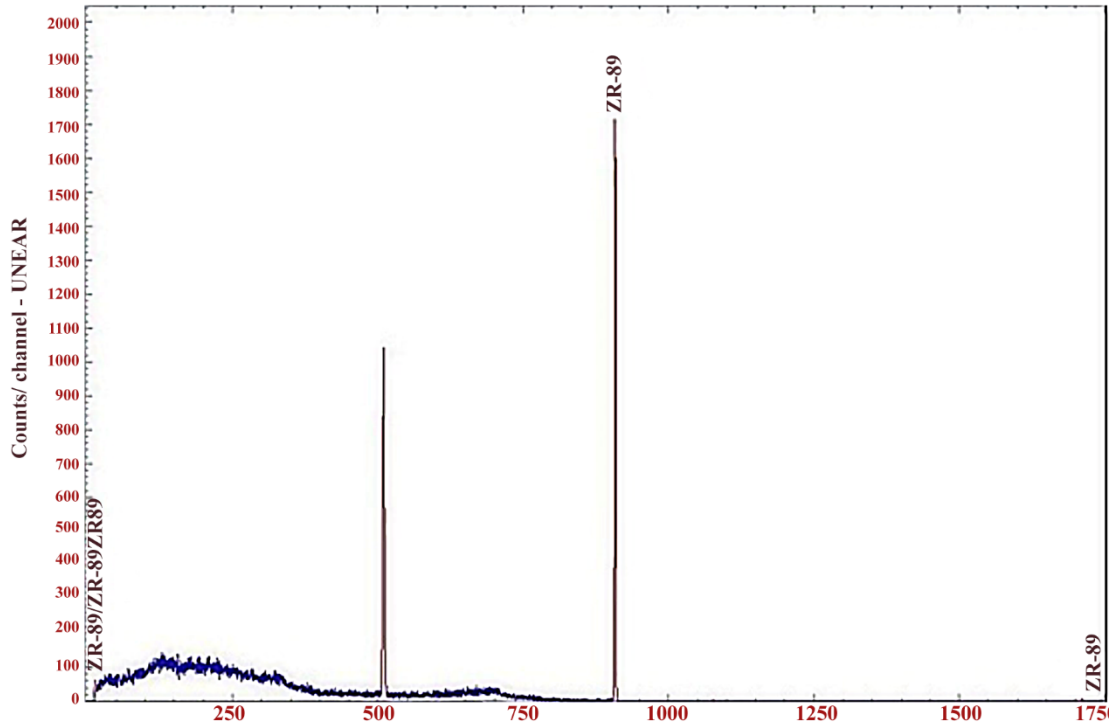

Fig 4. The gamma spectrum of the final [^{89}Zr]Zr-oxalate solution using a N-type coaxial HPGe detector. 511 keV gamma-rays produced in positron annihilation are seen in the spectrum

Chemical and radiochemical purities

The amount of metal ions in the final solution was determined by the ICP-OES method (Table 1). The total amount of the metal ions in the final solution was less than 0.1 ppm. The radiochemical purity was investigated by the ITLC method indicating purity of higher than 99% (Figure 5).

Table 1. Amount of metal ions in the final solution determined by ICP-OES method

Metal ion	Yttrium (target)	Aluminum (holder)
Impurity (ppm)	<0.1	<0.1

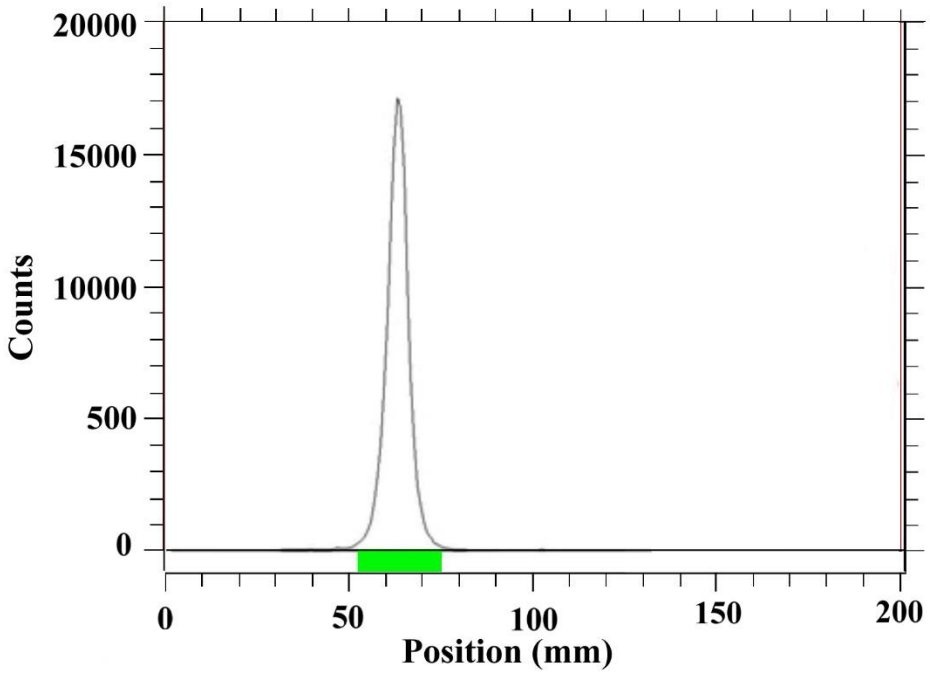

Fig 5. ITLC chromatogram of [^{89}Zr]Zr-oxalate solution using Whatman No.1 paper and 20 mM citric acid

Biodistribution studies of [^{89}Zr]Zr-oxalate in Wistar rats

The biodistribution of [^{89}Zr]Zr-oxalate in Wistar rats was studied for up to 48 h (Figure 6). As indicated, [^{89}Zr]Zr-oxalate is mainly accumulated in the bone. More activity is observed in the lung and heart compared to the other organs.

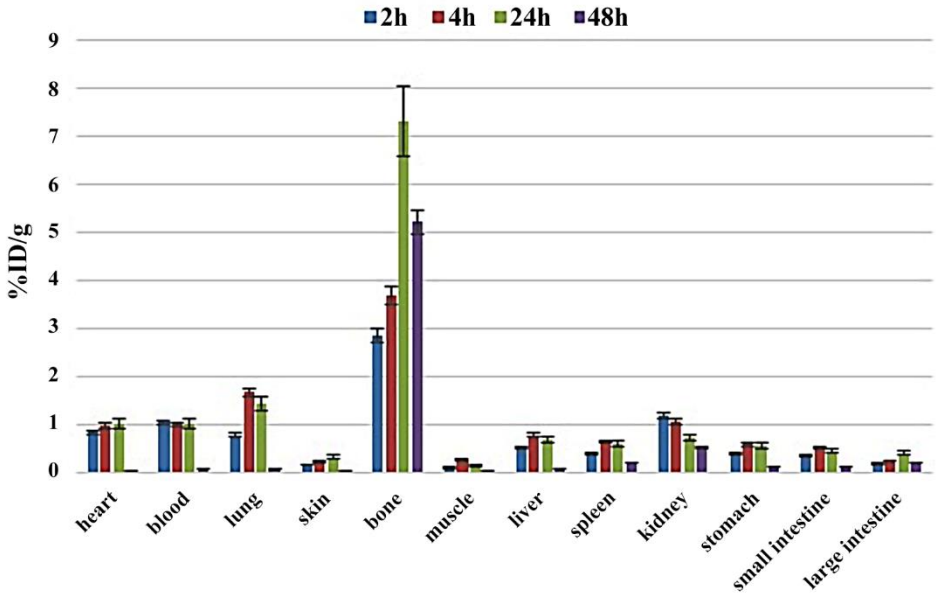

Fig 6. The injected dose per gram of [^{89}Zr]Zr-oxalate in Wistar rats at 2, 4, 24, and 48 h after injection

Imaging studies

The images of [^{89}Zr]Zr-oxalate biodistribution after 2, 24, 48, and 72 h of injection are presented in Figure 7. Accumulation of the activity in the bone is observed clearly.

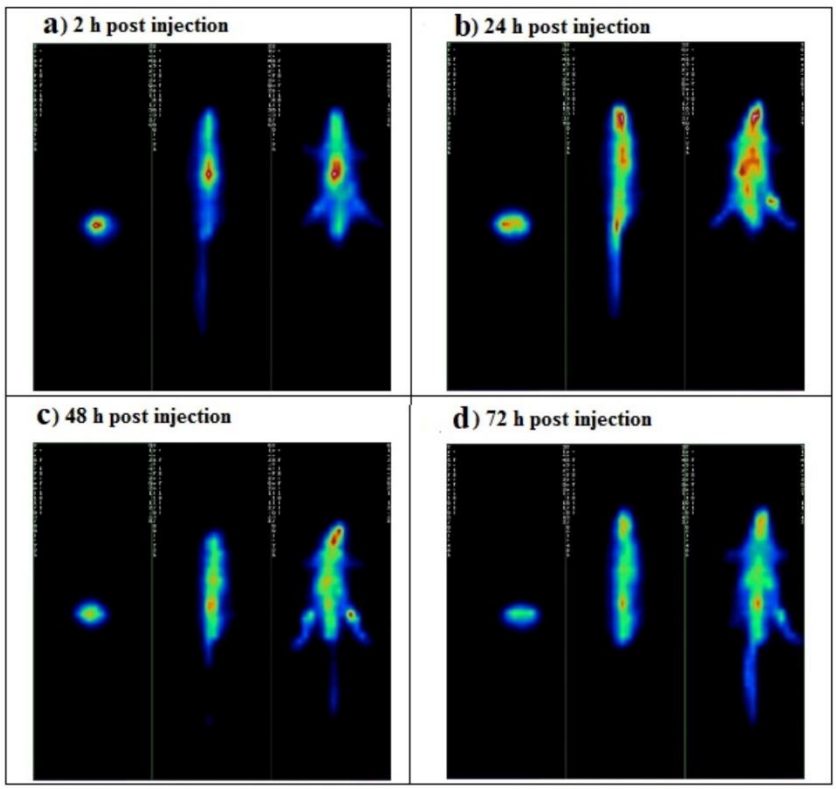

Fig 7. Scintigraphic images of Wistar rats after injection of [^{89}Zr]Zr-oxalate via their tail vein a) 2 h post injection; b) 24 h post injection; c) 48 h post injection; and d) 72 h post injection

Preparation and quality control of [^{89}Zr]Zr-DFO-trastuzumab

The radiochemical purity of the radiotracer was measured by the ITLC method using 20 mM citric acid (Figure 8). The radiochemical purity of the final solution was greater than 99 %. Also, the specific activity of the radiolabeled mAb was 74 GBq/g.

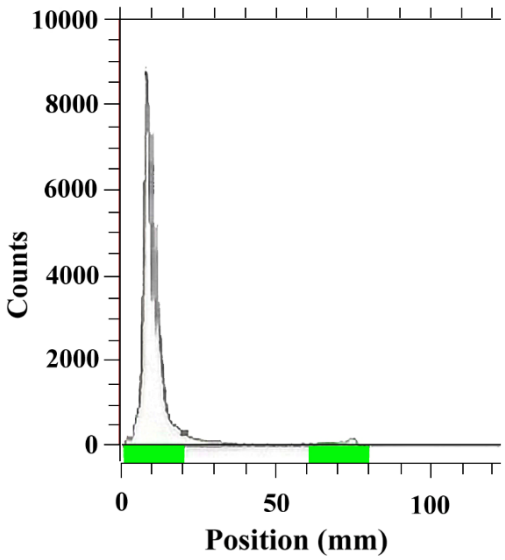

Fig 8. ITLC chromatogram of [^{89}Zr]Zr-DFO-trastuzumab using Whatman No.1 paper and 20 mM citric acid

DISCUSSION

In this study, ^{89}Y(p,n)^{89}Zr reaction was selected for ^{89}Zr production due to the availability of cyclotron and inexpensive production method (^{89}Y is 100% naturally abundant, and there is no need for the enriched targets). Production of ^{89}Zr from (p,n) reaction has been reported using Y foil targets, sputtered Y onto Cu and Y_2O_3 pellets. One of the main limitations of this study was the construction of a suitable target for the production of zirconium-89 with appropriate activity, which has not adequately explained in previous studies. While it seems that layering of yttrium on the copper backing in usual cyclotron targets is not a suitable and simple method, sputtering method produces a low level of activity. Therefore, in this study the use of Y_2O_3 pellets was considered as the available method to produce the target and to achieve the appropriate activity.

The cross-section of ^{89}Y(p,n)^{89}Zr reaction was determined using ALICE-91 and TALYS-1.8 codes at the energy range of 5-29 MeV. According to the results, the possible production of Rb, Sr, Y, and the other Zr radioisotopes also existed in this energy range. The data indicate that the production cross sections of most of these radioisotopes are zero in the energies below 15 MeV. However, the results of the codes were slightly different. As indicated in Figures 1 and 2, the cross-section of ^{88}Zr was equal to zero at the energies lower than 13 and 15 MeV by TALYS-1.8 and ALICE-91, respectively.

Besides, the maximum cross-section of ^{89}Zr was observed at 13 and 15 MeV energy from 0.86 to 0.93 b (Figure 3). Although, some discrepancy was observed between the data in the energy range of 13-19 MeV, the data were in good agreement between 5-13 MeV energy. According to these data, the energy of 13 to 15 MeV can be considered to achieve the higher production yield of ^{89}Zr and to avoid the production of ^{88}Zr and the other radioisotopes. While various studies have been performed on the production of ^{89}Zr through ^{89}Y(p,n)^{89}Zr reaction, the optimum proton energy was considered 12 to 18 MeV [9, 19-25].

In the current research, the incident energy of the proton was selected 14 MeV. The radionuclidic purity was investigated after the bombardment and after one month of production using an HPGe detector. As indicated in Figure 4, no contamination to ^{88}Zr and any other radionuclide were observed. After five hours bombardment with the current of 25 µA, 3260.34 MBq of ^{89}Zr was produced, resulting in the yield of 25.90±1.48 MBq/µA.h. While several studies have been reported on ^{89}Zr production using different targets, the yield of production is very different depending on the type and thickness of the target. The yield of ^{89}Zr production reported in the

various literature is presented in Table 2. The amount obtained in this study is similar to the results of kandil et al. research (28 MBq/μA. h), which also used Y_2O_3 pellets for the production [25].

Table 2. The yield of ^{89}Zr production reported in the previous literatures

Target	Yield	Ref
Y_2O_3 layer deposited on copper substrate	60.77 MBq/μA.h	[9]
^{89}Y-foil target (0.1 mm, 100% natural abundance)	207.94±15.17 MBq/μA·h	[24]
150 μm thick foil	8.83-15.56 MBq/μA.h	[26]
Y_2O_3 pellets	28 MBq/μA. h	[25]
Y_2O_3 pellets	25.90±1.48 MBq/μA.h.	Current study

Different techniques including solvent extraction, solid cation exchange, solid anion exchange, and hydroxamate resin have been reported for the separation of ^{89}Zr from the yttrium target and any other chemical impurities [19, 24-25, 27]. Hydroxamic acids have a high specific affinity for zirconium and form stable complexes [28]. Recently, it has been known as the preferred method for zirconium separation [24]. ZR-resin is the commercially available hydroxamate resin used here. The chemical purity of [^{89}Zr]Zr-oxalate solution was assessed by ICP-OES method after separation step, indicating less than 0.1 ppm impurity.

The high accumulation of the [^{89}Zr]Zr-oxalate was observed in the bone tissue both by biodistribution study and imaging process. Although, the increment of the bone uptake is observed up to 24 h, while it decreases afterward. This result is in complete agreement with other published data that has shown a considerable amount of ^{89}Zr accumulates in the bone marrow when various forms of ^{89}Zr including [^{89}Zr]Zr-chloride, [^{89}Zr]Zr-citrate, and [^{89}Zr]Zr-oxalate entered into the circulatory system. However, the main cause of the bone marrow uptake is unknown, but it has been suggested that ^{89}Zr bone uptake can be attributed to a metabolic process, as it seems to be more-pronounced for internalizing antibodies compared with noninternalizing antibodies [29-32]. The uptake of the heart and the lung were also high compared to the other organs, which are similar to Abou et al. report [29].

In this study, radiolabeling of trastuzumab with ^{89}Zr was performed only in two-step procedure approximately in 2 h. While several experiments were performed to achieve the best conditions for radiolabeling, the general process is similar to chang et al. report [18]. Slight modifications were observed in chelator/mAb and ^{89}Zr/mAb optimal ratios. The radiochemical purity was carried out using the RTLC method and 20 mM citric acid as the mobile phase. Whereas [^{89}Zr]Zr-DFO-trastuzumab remained at the origin, free [^{89}Zr]Zr-oxalate was observed at R_f =0.9 (Figure 8).

CONCLUSION

In this research study, ^{89}Zr was produced from the ^{89}Y(p,n)^{89}Zr reaction using a 30 MeV cyclotron. Five hours proton bombardment of $^{89}Y_2O_3$ pellet target with the current of 25 μA yield to 88.2±5.1 mCi of ^{89}Zr with the radionuclidic purity of higher than 99.99%. The total amount of metal ions in the solution was less than 0.1 ppm. [^{89}Zr]Zr-DFO-trastuzumab was successfully produced with radiochemical purity of higher than 99% and specific activity of 74 GBq/g. Generally, the results of this research confirmed that the possible production of the ^{89}Zr-based radioimmounopharmaceuticals with high purity and suitable activity using the produced radioisotope, which in turn can potentially lead to diagnostic as well as therapeutic tools specially for management of cancers.

Acknowledgment

The authors would like to acknowledge the invaluable scientific and financial support of International Atomic Energy Agency (IAEA) for this research under the Coordinated Research Project (Project Code; F22071).

REFERENCES

1. Burkhardt C, Bühler L, Viertl D, Stora T. New isotopes for the treatment of pancreatic cancer in collaboration with CERN: a mini review. Front Med (Lausanne). 2021 Aug 2;8:674656.
2. Klaassen NJM, Arntz MJ, Gil Arranja A, Roosen J, Nijsen JFW. The various therapeutic applications of the medical isotope holmium-166: a narrative review. EJNMMI Radiopharm Chem. 2019 Aug 5;4(1):19.
3. Marengo M, Lodi F, Magi S, Cicoria G, Pancaldi D, Boschi S. Assessment of radionuclidic impurities in 2-[18F] fluoro-2-deoxy-D-glucose ([18F] FDG) routine production. Appl Radiat Isot. 2008 Mar 1;66(3):295-302.
4. Lodi F, Rizzello A, Trespidi S, Di Pierro D, Marengo M, Farsad M, Fanti S, Al-Nahhas A, Rubello D, Boschi S. Reliability and reproducibility of N-[11C] methyl-choline and L-(S-methyl-[11C]) methionine solid-phase synthesis:

a useful and suitable method in clinical practice. Nucl Med Commun. 2008 Aug 1;29(8):736-40.
5. Jalilian AR. An overview on Ga-68 radiopharmaceuticals for positron emission tomography applications. Iran J Nucl Med. 2016;24(1):1.
6. Chomet M, van Dongen GAMS, Vugts DJ. State of the art in radiolabeling of antibodies with common and uncommon radiometals for preclinical and clinical immuno-PET. Bioconjug Chem. 2021 Jul 21;32(7):1315-1330.
7. Dammes N, Peer D. Monoclonal antibody-based molecular imaging strategies and theranostic opportunities. Theranostics. 2020 Jan 1;10(2):938-955.
8. Chu SYF, Ekström LP, Firestone RB. Table of radioactive isotopes. Accessed September 9, 2022. Available from: http://nucleardata.nuclear.lu.se/toi/nuclide.asp?iZA=400089
9. Sadeghi M, Enferadi M, Bakhtiari M. Accelerator production of the positron emitter zirconium-89. Ann Nucl Energy. 2012 Mar 1;41:97-103.
10. Deri MA, Zeglis BM, Francesconi LC, Lewis JS. PET imaging with ^{89}Zr: from radiochemistry to the clinic. Nucl Med Biol. 2013 Jan;40(1):3-14.
11. Severin GW, Engle JW, Barnhart TE, Nickles RJ. 89Zr radiochemistry for positron emission tomography. Med Chem. 2011 Sep;7(5):389-94.
12. Zakaly HMH, Mostafa MYA, Zhukovsky M. Biokinetic modelling of 89Zr-labelled monoclonal antibodies for dosimetry assessment in humans. Int J Radiat Res. 2020 Oct;18(4):825-833.
13. van de Watering FC, Rijpkema M, Perk L, Brinkmann U, Oyen WJ, Boerman OC. Zirconium-89 labeled antibodies: a new tool for molecular imaging in cancer patients. Biomed Res Int. 2014;2014:203601.
14. Jauw YW, Menke-van der Houven van Oordt CW, Hoekstra OS, Hendrikse NH, Vugts DJ, Zijlstra JM, Huisman MC, van Dongen GA. Immuno-positron emission tomography with zirconium-89-labeled monoclonal antibodies in oncology: what can we learn from initial clinical trials? Front Pharmacol. 2016 May 24;7:131.
15. Sharifian M, Sadeghi M, Alirezapour B, Yarmohammadi M, Ardaneh K. Modeling and experimental data of zirconium-89 production yield. Appl Radiat Isot. 2017 Dec;130:206-210.
16. Kasbollah A, Eu P, Cowell S, Deb P. Review on production of 89Zr in a medical cyclotron for PET radiopharmaceuticals. J Nucl Med Technol. 2013 Mar;41(1):35-41.
17. Currie, L. Quantifying uncertainty in nuclear analytical measurements. IAEA-TECDOC-1401**.** Accessed September 9, 2022. Available from: https://www.nist.gov/publications/quantifying-uncertainty-nuclear-analytical-measurements
18. Chang AJ, Desilva R, Jain S, Lears K, Rogers B, Lapi S. 89Zr-radiolabeled trastuzumab imaging in orthotopic and metastatic breast tumors. Pharmaceuticals (Basel). 2012 Jan 5;5(1):79-93.
19. Wooten AL, Madrid E, Schweitzer GD, Lawrence LA, Mebrahtu E, Lewis BC, Lapi SE. Routine production of 89Zr using an automated module. Appl Sci.. 2013 Jul 12;3(3):593-613.
20. Mansel A, Franke K. Production of no-carrier-added 89Zr at an 18 MeV cyclotron, its purification and use in investigations in solvent extraction. J Radioanal Nucl Chem. 2021 Apr;328(1):419-23.
21. Uddin MS, Hagiwara M, Baba M, Tarkanyi F, Ditroi F. Experimental studies on excitation functions of the proton-induced activation reactions on yttrium. Appl Radiat Isot. 2005 Sep;63(3):367-74.
22. Omara HM, Hassan KF, Kandil SA, Hegazy FE, Saleh ZA. Proton induced reactions on 89Y with particular reference to the production of the medically interesting radionuclide 89Zr. Radiochim Acta. 2009 Aug 1;97(9):467-71.
23. Hohn A, Zimmermann K, Schaub E, Hirzel W, Schubiger PA, Schibli R. Production and separation of ''non-standard'' PET nuclides at a large cyclotron facility: the experiences at the Paul Scherrer Institute in Switzerland. Q J Nucl Med Mol Imaging. 2008 Jun;52(2):145-50. Epub 2008 Jan 5.
24. Holland JP, Sheh Y, Lewis JS. Standardized methods for the production of high specific-activity zirconium-89. Nucl Med Biol. 2009 Oct;36(7):729-39.
25. Kandil SA, Scholten B, Saleh ZA, Youssef AM, Qaim SM, Coenen HH. A comparative study on the separation of radiozirconium via ion-exchange and solvent extraction techniques, with particular reference to the production of 88Zr and 89Zr in proton induced reactions on yttrium. J Radioanal Nucl Chem. 2007 Oct;274(1):45-52.
26. Dabkowski AM, Probst K, Marshall C. Cyclotron production for the radiometal Zirconium-89 with an IBA cyclone 18/9 and COSTIS solid target system (STS). AIP Conf Proc. 2012 Dec 19; 1509(1): 108-113.
27. Larenkov A, Bubenschikov V, Makichyan A, Zhukova M, Krasnoperova A, Kodina G. Preparation of Zirconium-89 solutions for radiopharmaceutical purposes: interrelation between formulation, radiochemical purity, stability and biodistribution. Molecules. 2019 Apr 18;24(8):1534.
28. Baroncelli F, Grossi G. The complexing power of hydroxamic acids and its effect on the behaviour of organic extractants in the reprocessing of irradiated fuels—I the complexes between benzohydroxamic acid and zirconium, iron (III) and uranium (VI). J inorg nucl chem. 1965 May 1;27(5):1085-92.
29. Abou DS, Ku T, Smith-Jones PM. In vivo biodistribution and accumulation of 89Zr in mice. Nucl Med Biol. 2011 Jul;38(5):675-81. doi: 10.1016/j.nucmedbio.2010.12.011. Epub 2011 Mar 3.
30. Heskamp S, Raavé R, Boerman O, Rijpkema M, Goncalves V, Denat F. ^{89}Zr-Immuno-positron emission tomography in oncology: state-of-the-art ^{89}Zr radiochemistry. Bioconjug Chem. 2017 Sep 20;28(9):2211-2223.
31. Holland JP, Divilov V, Bander NH, Smith-Jones PM, Larson SM, Lewis JS. 89Zr-DFO-J591 for immunoPET of prostate-specific membrane antigen expression in vivo. J Nucl Med. 2010 Aug;51(8):1293-300.
32. Laverman P, van der Geest T, Terry SY, Gerrits D, Walgreen B, Helsen MM, Nayak TK, Freimoser-Grundschober A, Waldhauer I, Hosse RJ, Moessner E, Umana P, Klein C, Oyen WJ, Koenders MI, Boerman OC. Immuno-PET and immuno-SPECT of rheumatoid arthritis with radiolabeled anti-fibroblast activation protein antibody correlates with severity of arthritis. J Nucl Med. 2015 May;56(5):778-83.